Mathematical Biosciences and Engineering

https://www.aimspress.com/journal/mbe

MBE, 23(11): 3415–3435.
DOI: 10.3934/mbe.2026117
Received: 20 May 2026
Revised: 30 September 2026
Accepted: 28 October 2026
Published: 18 November 2026

Research article

Parameter estimation in generalized fractional neuronal models

Pauliina Ilmonen[1], Milla Laurikkala[1*], Enrica Pirozzi[2], Luigia Caputo[3] and Lauri Viitasaari[4]

[1] Aalto University School of Science, Department of Mathematics and Systems Analysis, PO Box 11100, 00076 Aalto, Finland

[2] Department of Mathematics and Physics, University of Campania Luigi Vanvitelli, Caserta, 81100, Italy

[3] Department of Mathematics and Applications, University of Naples Federico II, Naples, 80126, Italy

[4] Aalto University School of Business, Department of Information and Service Management, PO Box 21210, 00076 Aalto, Finland

* **Correspondence:** Email: milla.laurikkala@aalto.fi; Tel: +358-50-3303146.

Abstract: We investigate a generalized stochastic fractional neuronal model combining fractional dynamics with correlated stochastic inputs. The proposed framework is described by a fractional differential equation driven by a latent stochastic process with stationary increments and mean-reverting structure. This formulation allows the inclusion of both short-range and long-range dependence structures and naturally produces non-exponential relaxation phenomena. The main goal is the development of a feasible parameter estimation procedure based on discrete observations of the neuronal state process. We propose a two-step methodology. First, the parameters governing the fractional dynamics are estimated by exploiting the asymptotic behavior of Mittag–Leffler functions near the origin. Subsequently, the latent stochastic input is reconstructed through fractional differentiation techniques, allowing the estimation of the parameters governing the hidden noise dynamics. We derive quantitative error bounds for the estimators and analyze the reconstruction error of the latent process under suitable regularity assumptions on the driving noise. In particular, the interplay between the order of the fractional derivative and the Hölder regularity of the noise process naturally emerges in the stability analysis of the reconstruction procedure. Finally, simulation studies illustrate the applicability of the proposed methodology and highlight the influence of memory effects and noise regularity on the quality of statistical inference. The results support the relevance of fractional stochastic analysis for the modeling and inference of neuronal systems with memory and correlated inputs.

Keywords: neuronal modeling; parameter estimation; non-Markovian dynamics; noise reconstruction

1. Introduction

The mathematical modeling of neuronal activity has a long and rich history, spanning biophysical, probabilistic, and more recently fractional-calculus-based approaches. Classically, models are based on Markovian structures, see monograph [1] and a survey [2], or article [3] for a broader overview of mathematical modeling of brain dynamics. Recently, however, the mathematical modeling of neuronal activity has progressively evolved from purely Markovian frameworks toward nonlocal and memory-dependent formulations. The reason behind this is the experimental evidence indicating that neuronal systems exhibit persistent temporal correlations, hereditary effects, adaptation mechanisms, and anomalous relaxation phenomena that cannot be adequately described by classical stochastic differential equations driven by white noise. This has motivated the introduction of stochastic models based on fractional calculus, which have gained increasing attention in the description of complex biological systems where memory effects and nonlocal dynamics play a fundamental role. A systematic treatment of fractional calculus in bioengineering is given in [4]. Fractional constitutive laws for linear viscoelastic media with Mittag–Leffler type relaxation were developed in [5], and on the probabilistic side, Meerschaert and Sikorskii [6] showed how fractional derivatives arise as governing equations for scaling limits of continuous time random walks. A fractional approach to anomalous diffusion was reviewed in [7].

Fractional derivatives, and in particular the Caputo derivative, provide a convenient mathematical tool to incorporate such memory effects into dynamical systems. In this framework, the evolution of the system depends not only on its current state but also on its entire past history, allowing for a more realistic modeling of biological phenomena. This perspective has been successfully adopted in several contexts, including anomalous diffusion, viscoelasticity, and mathematical neuroscience [8, 9]. Teka, Marinov and Santamaria [9] proposed a fractional leaky integrate-and-fire model in which varying only the fractional exponent reproduces memory effects which the classical integrate-and-fire model cannot reproduce. Pirozzi [8] modeled neuronal dynamics on different time scales through two coupled fractional stochastic differential equations with different fractional orders, one for the membrane potential and one for the correlated input.

In the context of neuronal modeling, fractional stochastic dynamics were investigated in [10], where a model driven by colored noise was introduced to describe correlated synaptic inputs and adaptation effects in neuronal firing activity. That model already demonstrated that fractional dynamics naturally produce non-exponential relaxation and persistent correlations consistent with experimentally observed neuronal behavior. Subsequently, the class of fractionally integrated stochastic processes was further developed in [11, 12]. Abundo and Pirozzi [11] studied Riemann–Liouville fractional integrals of Gauss–Markov processes, and Pirozzi [12] introduced the Mittag–Leffler fractional stochastic process, which appears in the solutions of coupled fractional SDEs. The processes introduced therein generalize classical Gauss–Markov and Ornstein–Uhlenbeck dynamics by replacing the exponential kernel with Mittag–Leffler type kernels arising from fractional integration, providing analytically tractable models with explicit covariance structures and long-memory properties.

A complementary and closely related framework is provided by time-changed stochastic processes, typically constructed via inverse subordinators, which lead to non-Markovian dynamics with heavy-tailed waiting times and long-range dependence [13]. These processes offer a flexible framework to model subdiffusive behaviors and complex temporal structures, and have been applied to biological

systems to capture temporal patterns arising in intracellular dynamics and neuronal activity [14]. In particular, the combination of fractional integration and stochastic time changes leads to models that naturally exhibit both long memory and non-exponential relaxation.

Despite this growing literature, parameter estimation for neuronal systems with latent stochastic inputs remains a challenging and largely open problem. The main difficulty lies in the simultaneous presence of three features: (i) fractional dynamics, (ii) partially observed systems, and (iii) general noise structures deviating from classical Brownian motion. In this article, we consider a generalized neuronal model of the form

$$D^\alpha V_t = AV_t + \eta(t),$$

where D^α denotes the Caputo fractional derivative, and the stochastic input $\eta(t)$ is modeled as a mean-reverting process satisfying

$$d\eta(t) = \Theta(b - \eta(t))\, dt + \sigma\, dG_t,$$

with G a stochastic process with stationary increments. This formulation extends classical neuronal models by allowing for both fractional dynamics in the membrane potential and a flexible class of driving noises [8], and can be simultaneously viewed as a generalized fractional neuronal model extending [8,10], as a generalized fractionally integrated stochastic system in the spirit of [11,12], and as a non-Markovian neuronal model with latent correlated stochastic input. The stochasticity arises from the generalized Ornstein–Uhlenbeck model for the noise η that acts as the random noise for the system describing observed V. The memory effect can be incorporated to the model via two mechanisms; 1) through non-local fractional derivative D^α incorporating memory of V; and 2) through random noise η that can possess arbitrary memory structures via driving noise dG_t that essentially is simply assumed to have stationary increments.

Our main goal is to develop a feasible parameter estimation procedure for unknown $(\alpha, A, b, \Theta, \sigma)$ from the observations V. Our approach follows a natural two-step strategy: first, we estimate the parameters (α, A) governing the fractional dynamics by exploiting the small-time asymptotic properties of the solution expressed in terms of Mittag–Leffler functions; and after parameters A and α are recovered, we reconstruct the latent process η and estimate the parameters of its dynamics by using well-established procedures for parameter estimation in Ornstein–Uhlenbeck models, see [15] and references therein for the multivariate Langevin equation, and [16] for parameter estimation in the generalized multivariate Vasicek model. In particular, if η can be accurately reconstructed, then we can follow non-parametric approaches presented in [16] for the estimation of (b, Θ, σ). As our main findings, we show that parameters (α, A) can be recovered from observations V by dense observations in small-time asymptotics, allowing to recover latent noise η. After that, one can follow procedures described in [16] to recover parameters of the stationary η by controlling the error one makes in recovering (a priori unobserved) η.

Our contribution is twofold: first, we introduce a generalized fractional neuronal model that encompasses several existing approaches as special cases; and second, we propose a practical estimation procedure allowing us to simultaneously estimate all parameters by combining small- and large-time asymptotics. To the best of our knowledge, there are no existing procedures that would estimate all parameters of the generalized fractional neuronal model.

The rest of the paper is organized as follows: in Section 2, we introduce our model and define our estimation procedure together with our main theorems providing quantitative error bounds for

the estimators; in Section 3, we illustrate our procedure via numerical examples highlighting both its effectiveness and its limitations; and we end the paper with short discussions in Section 4.

2. Theoretical approach

The model is defined via the following equations:

$$\begin{aligned} D^\alpha V_t &= AV_t + \eta(t), \qquad V(0) = V_0, \\ d\eta(t) &= \Theta(b - \eta(t))dt + \sigma dG_t, \qquad \eta(0) = 0, \end{aligned} \tag{2.1}$$

where $\alpha \in (0,1), A, b, \Theta \in \mathbb{R}$. Here, $D^\alpha f$ denotes the Caputo fractional derivative defined as follows (e.g., see [13]):

$$D^\alpha f(t) = \frac{1}{\Gamma(1-\alpha)} \int_0^t f'(\tau)(t-\tau)^{-\alpha} d\tau. \tag{2.2}$$

The fractional order α determines the memory of V: values close to 1 correspond to shorter memory and smaller values correspond to longer memory and slower relaxation. The parameter A describes the characteristic time of the membrane, including the membrane capacitance and leak conductance [12]. The parameters b, Θ, and σ are related to the latent noise process, with b representing the long-term mean of η, Θ modeling its mean reversion effect, and σ describing the intensity or amplitude of the noise.

Without loss of generality, we assume $V_0 = 1$ for notational simplicity. Moreover, we assume $A < 0$, referring to the Leaky Integrate-and-Fire (LIF) neuronal model based on the stochastic version of the Langevin equation, [17]. The solution V is given by the following (see [12]):

$$V_t = E_\alpha(t^\alpha A) + \int_0^t s^{\alpha-1} E_{\alpha,\alpha}(s^\alpha A)\eta(t-s)ds, \quad \forall t > 0, \quad V_0 = 1. \tag{2.3}$$

Here, $E_{\alpha,\beta}$ is the two-parameter Mittag-Leffler function given by

$$E_{\alpha,\beta}(z) = \sum_{k=0}^{\infty} \frac{z^k}{\Gamma(\alpha k + \beta)} \tag{2.4}$$

and $E_\alpha(z) = E_{\alpha,1}(z)$. From (2.4), we obtain asymptotic behavior at zero given by

$$E_{\alpha,\beta}(x) \sim \frac{1}{\Gamma(\beta)} + \frac{x}{\Gamma(\alpha+\beta)},$$

and in particular $E_\alpha(x) \sim 1 + \frac{x}{\Gamma(1+\alpha)}$. This motivates the following definition.

Definition 2.1. *We set*

$$\hat{\alpha} = I_{V_{2t}<1, V_t<1} \frac{\log(1 - V_{2t}) - \log(1 - V_t)}{\log 2} \tag{2.5}$$

with the convention $\hat{\alpha} = 0$ *if* $I_{V_{2t}<1,V_t<1} = 0$ *and*

$$\hat{A} = \Gamma(1+\hat{\alpha}) t^{-\hat{\alpha}} (V_t - 1). \tag{2.6}$$

Remark 2.2. In practice, the estimators can be computed by regressing $\log(1 - V_t)$ against $\log t$ and using the asymptotics

$$\log(1 - V_t) \sim \alpha \log t + \log\left[\frac{|A|}{\Gamma(1+\alpha)}\right], \tag{2.7}$$

as we have done in Section 3.1. This provides more stable estimators as the asymptotics $t \to 0$ becomes numerically unstable due to discretization errors. We note that the regression approach would also be feasible in practical applications with more sparsely sampled observations. Indeed, when regressing $\log(1 - V_t)$ against $\log t$, an arbitrarily small t is not required. Instead, all times t used in the regression should be sufficiently close to zero so that the asymptotic behavior of V is still captured. This leads to a natural trade-off between the number of data points required for regression and the error that (2.7) makes.

Once the parameters α and A are recovered, one can retrieve the noise process η from $\eta(t) = D^\alpha V_t - AV_t$, motivating noise recovery via $\hat{\eta}(t) = D^{\hat{\alpha}} V_t - \hat{A} V_t$. In order to further stabilize this against numerical errors arising from the discretised fractional derivative (3.1), we subtract the deterministic part and use

$$\hat{\eta}(t) = D^{\hat{\alpha}}\left[V_t - E_{\hat{\alpha}}(\hat{A}t^{\hat{\alpha}})\right] - \hat{A}\left[V_t - E_{\hat{\alpha}}(\hat{A}t^{\hat{\alpha}})\right]. \tag{2.8}$$

This is valid since $D^{\hat{\alpha}} E_{\hat{\alpha}}(\hat{A}t^{\hat{\alpha}}) = \hat{A} E_{\hat{\alpha}}(\hat{A}t^{\hat{\alpha}})$. If $\hat{\eta}$ is not too far from the true noise η, then the parameters (b, Θ, σ) can be recovered exactly as in [16]. More precisely, controlling the error $|\hat{\eta}(t) - \eta(t)|$ allows us to base the estimators of (b, Θ, σ) on $\hat{\eta}$ instead of η. Then, the growth of the error $|\hat{\eta}(t) - \eta(t)|$ (as the time window T required for the estimation increases) has to be compensated by better estimation of α and A.

Our first main result, Theorem 2.3 below, provides a precise error analysis on the estimation of α and A on small-time asymptotics. Our second main theorem, Theorem 2.4 below, provides quantitative error bounds for the estimation of the noise term $\hat{\eta}$ given in terms of the estimation error of α and A. Combined with the exact rates of convergence for the estimators of (b, Θ, σ) provided in [16], together with the error rates in Theorem 2.3, one can now easily deduce how accurately α and A must be estimated on small-time asymptotics in order to have a small enough error for $|\hat{\eta} - \eta|$ when T is large, which is required for accurate estimation of (b, Θ, σ).

Theorem 2.3. *Suppose that η is almost surely Hölder continuous of order $\gamma \in (\alpha, 1)$. Then there exist random variables $t_0 = t_0(\omega) \in (0, 1]$ and $C = C_\omega$, where C_ω only depends on A, α, γ, and the Hölder constant of η on $[0, 1]$, such that, for all $t \in (0, t_0]$, the following hold:*

1. *We have*
$$|\hat{\alpha} - \alpha| \le C_\omega t^\alpha. \tag{2.9}$$
In particular, $\hat{\alpha} \to \alpha$ almost surely as $t \to 0$.
2. *We have*
$$|\hat{A} - A| \le C_\omega t^\alpha |\log t|. \tag{2.10}$$
In particular, $\hat{A} \to A$ almost surely as $t \to 0$.

Proof. In the following, C_ω denotes a random constant that might depend on A, α, γ, and ω, but is independent of $t \in [0, 1]$. We write

$$1 - V_t = \frac{-At^\alpha}{\Gamma(1+\alpha)} - E(t) \tag{2.11}$$

with

$$E(t) = E_\alpha(t^\alpha A) - \frac{At^\alpha}{\Gamma(1+\alpha)} + \int_0^t s^{\alpha-1} E_{\alpha,\alpha}(s^\alpha A)\eta(t-s)ds.$$

First, we prove an upper bound for $E(t)$. For this, we get from (2.4) that

$$\left| E_\alpha(t^\alpha A) - 1 - \frac{At^\alpha}{\Gamma(1+\alpha)} \right| \le Ct^{2\alpha}. \tag{2.12}$$

For the random part, Hölder continuity of η together with $\eta(0) = 0$ implies the following:

$$\begin{aligned} &\left| \int_0^t s^{\alpha-1} E_{\alpha,\alpha}(s^\alpha A)\eta(t-s)ds \right| \le C_\omega \int_0^t s^{\alpha-1}(t-s)^\gamma ds \\ &\le C_\omega t^{\gamma+\alpha} \le C_\omega t^{2\alpha}. \end{aligned}$$

Combining the above estimates gives us the following:

$$|E(t)| \le (C + C_\omega)t^{2\alpha}. \tag{2.13}$$

This, in particular, implies that there exists $t_0 = t_0(\omega)$ such that, for all $t \le t_0$, we have

$$|E(t)| \le \frac{-At^\alpha}{2\Gamma(1+\alpha)}, \tag{2.14}$$

which, in turn, implies

$$1 - V_t = \left[\frac{-A}{\Gamma(1+\alpha)} - \frac{E(t)}{t^\alpha} \right] t^\alpha > 0.$$

Consequently, for $t \le \frac{t_0}{2}$ we have, almost surely, that

$$\hat{\alpha} = \frac{\log(1 - V_{2t}) - \log(1 - V_t)}{\log 2}.$$

Here, note that

$$\begin{aligned} \log(1 - V_t) &= \log\left[\frac{-At^\alpha}{\Gamma(1+\alpha)} - E(t) \right] \\ &= \log\left[\frac{-A}{\Gamma(1+\alpha)} \right] + \alpha \log t + \log\left[1 + \frac{\Gamma(1+\alpha)E(t)}{At^\alpha} \right]. \end{aligned}$$

Similarly, we obtain

$$\begin{aligned} \log(1 - V_{2t}) &= \log\left[\frac{-A(2t)^\alpha}{\Gamma(1+\alpha)} - E(2t) \right] \\ &= \log\left[\frac{-A}{\Gamma(1+\alpha)} \right] + \alpha \log 2 + \alpha \log t + \log\left[1 + \frac{\Gamma(1+\alpha)E(2t)}{A(2t)^\alpha} \right], \end{aligned}$$

leading to

$$|\hat{\alpha} - \alpha| = \left| \frac{\log(1 - V_{2t}) - \log(1 - V_t)}{\log 2} - \alpha \right|$$

$$= \left|\log\left[1 + \frac{\Gamma(1+\alpha)E(2t)}{A(2t)^\alpha}\right] - \log\left[1 + \frac{\Gamma(1+\alpha)E(t)}{At^\alpha}\right]\right|$$
$$\leq \left|\log\left[1 + \frac{\Gamma(1+\alpha)E(2t)}{A(2t)^\alpha}\right]\right| + \left|\log\left[1 + \frac{\Gamma(1+\alpha)E(t)}{At^\alpha}\right]\right|.$$

Now, (2.14) and $t \leq \frac{t_0}{2}$ allow us to use $|\log(1+x)| \leq \frac{3}{2}|x|$ for $|x| \leq \frac{1}{2}$. This, together with (2.13), gives an estimate

$$|\hat{\alpha} - \alpha| \leq C_\omega t^\alpha,$$

which proves (2.9). For (2.10), we use (2.11) and (2.6) to obtain the following:

$$\hat{A} - A = \left[\frac{\Gamma(1+\hat{\alpha})t^\alpha}{\Gamma(1+\alpha)t^{\hat{\alpha}}} - 1\right]A + \frac{\Gamma(1+\hat{\alpha})}{t^{\hat{\alpha}}}E(t)$$
$$= \left[\frac{\Gamma(1+\hat{\alpha})}{\Gamma(1+\alpha)} - 1\right]t^{\alpha-\hat{\alpha}}A + \left[t^{\alpha-\hat{\alpha}} - 1\right]A + \frac{\Gamma(1+\hat{\alpha})}{t^{\hat{\alpha}}}E(t).$$

First, we analyze $t^{\alpha-\hat{\alpha}}$ and provide a rate at which it converges to a constant 1. Using (2.9) allows us to estimate the following:

$$\left|t^{\alpha-\hat{\alpha}} - 1\right| = \left|e^{(\alpha-\hat{\alpha})\log t} - 1\right| \leq e^{|\alpha-\hat{\alpha}||\log t|} - 1 \leq e^{C_\omega t^\alpha |\log t|} - 1$$
$$\leq C_\omega t^\alpha |\log t| e^{C_\omega t^\alpha |\log t|} \leq C_\omega t^\alpha |\log t|.$$

Moreover, using the smoothness of $\Gamma(1+x)$ around $x = \alpha$ and (2.13) immediately yields for the last two terms that

$$\left[t^{\alpha-\hat{\alpha}} - 1\right]A + \frac{\Gamma(1+\hat{\alpha})}{t^{\hat{\alpha}}}E(t) \leq C_\omega t^\alpha |\log t| + C_\omega t^\alpha t^{\alpha-\hat{\alpha}} \leq C_\omega t^\alpha |\log t|.$$

Similarly, using the smoothness of the Gamma function $\Gamma(x)$, we deduce that

$$\left[\frac{\Gamma(1+\hat{\alpha})}{\Gamma(1+\alpha)} - 1\right]t^{\alpha-\hat{\alpha}}A \leq C_\omega|\alpha - \hat{\alpha}| \leq C_\omega t^\alpha.$$

Combining all the estimates leads to (2.10) and completes the whole proof. □

By Theorem 2.3, we can recover α and A with arbitrary precision by zooming in to short-time asymptotics. In order to estimate (b, Θ, σ), note that σ can also be estimated with arbitrary precision on short time asymptotics if η can be recovered, see [16]. On the other hand, the estimation of (b, Θ) is based on long periods $[0, T]$ with $T \to \infty$ allowing for an accurate estimation of the mean and covariances of an (asymptotically) stationary series η. For this purpose, one also needs the control of the error $|\hat{\eta} - \eta|$ that is the topic of the next theorem.

In the sequel, we use notation $f \lesssim g$ if $|f| \leq C|g|$ for some unimportant constant C independent of T, but possibly depending on true parameters $(\alpha, A, b, \Theta, \sigma)$. Additionally, we note that as the time interval $[0, e]$ is dedicated to the estimation of parameters (α, A), the noise recovery is considered after the time period $[0, e]$ in the following.

Theorem 2.4. *Suppose that η is almost surely Hölder continuous of order $\gamma \in (\alpha, 1)$ and that $A < 0$. Let $\hat{\eta}$ be given by* (2.8)*. Then, for any fixed $T > e$, we have the following:*

$$\sup_{1\le t\le T} |\hat{\eta}(t) - \eta(t)| \lesssim (1 + C_T^{\eta} T^{\gamma-\alpha}) \log T |\alpha - \hat{\alpha}| + (1 + \|\eta\|_{T,\infty})|A - \hat{A}|,$$

where C_T^{η} is the Hölder constant of η on $[0, T]$.

For the proof, we write $V_t = E_\alpha(At^\alpha) + f(t)$ with

$$f(t) := \int_0^t (t-s)^{\alpha-1} E_{\alpha,\alpha}(A(t-s)^\alpha)\eta(s)ds \tag{2.15}$$

as the random part of V_t. The following lemma collects regularity properties of f. We denote the supremum norm on $[0, T]$ by $\|g\|_{\infty,T} := \sup_{0\le T} |g(t)|$.

Lemma 2.5. *Let $A < 0$, and suppose that η with $\eta(0) = 0$ is Hölder continuous of order $\gamma \in (\alpha, 1)$ on $[0, T]$. Let f be given by* (2.15)*. Then, $\|f\|_{\infty,T} \le \frac{\|\eta\|_{\infty,T}}{|A|}$ and, for all $s, t \in [0, T]$,*

$$|f(t) - f(s)| \le \frac{2C_T^{\eta}}{|A|}|t - s|^{\gamma},$$

where C_T^{η} is the Hölder constant of η on $[0, T]$.

Proof. Starting from the elementary identity $D^\mu E_\alpha(At^\alpha) = At^{\alpha-\mu}E_{\alpha,\alpha+1-\mu}(At^\alpha)$, we see $\frac{d}{du}E_\alpha(Au^\alpha) = Au^{\alpha-1}E_{\alpha,\alpha}(Au^\alpha)$. From monotonicity of $E_\alpha(At^\alpha)$, see e.g., [18] and facts $E_\alpha(0) = 1$ and $E_\alpha(-x) \to 0$ as $x \to \infty$ it follows that $u^{\alpha-1}E_{\alpha,\alpha}(Au^\alpha) \ge 0$ and $\int_0^\infty u^{\alpha-1}E_{\alpha,\alpha}(Au^\alpha)du = 1/|A|$. The first claim $\|f\|_{\infty,T} \le \frac{\|\eta\|_{\infty,T}}{|A|}$ directly follows from this. For the second, let $s < t$. Then,

$$f(t) - f(s) = \int_0^s u^{\alpha-1}E_{\alpha,\alpha}(Au^\alpha)\left[\eta(t-u) - \eta(s-u)\right]du + \int_s^t u^{\alpha-1}E_{\alpha,\alpha}(Au^\alpha)\left[\eta(t-u) - \eta(0)\right]du.$$

Here, $|\eta(t-u) - \eta(s-u)| + |\eta(t-u) - \eta(0)| \le 2C_T^{\eta}$, from which the second claim follows. This completes the whole proof. □

Proof of Theorem 2.4. We can decompose the following:

$$\begin{aligned}\hat{\eta}(t) - \eta(t) &= (D^{\hat{\alpha}} - D^\alpha)E_\alpha(At^\alpha) + (D^{\hat{\alpha}} - D^\alpha)f(t) + (A - \hat{A})E_\alpha(At^\alpha) + (A - \hat{A})f(t)\\ &=: I_1(t) + I_2(t) + I_3(t) + I_4(t).\end{aligned} \tag{2.16}$$

Since $A < 0$, we have $0 < E_\alpha(At^\alpha) \le 1$, and hence $|I_3(t)| \le |A - \hat{A}|$. Similarly, by the first part of Lemma 2.5, we get $|I_4(t)| \lesssim |A - \hat{A}|\|\eta\|_{\infty,T}$. It remains to estimate the terms $I_1(t)$ and $I_2(t)$. We begin with $I_1(t)$. Using $D^\mu E_\alpha(At^\alpha) = At^{\alpha-\mu}E_{\alpha,\alpha+1-\mu}(At^\alpha)$ again leads to the following:

$$\begin{aligned}I_1(t) &= At^{\alpha-\hat{\alpha}}E_{\alpha,\alpha+1-\hat{\alpha}}(At^\alpha) - AE_\alpha(At^\alpha)\\ &= A\Big(t^{\alpha-\hat{\alpha}} - 1\Big)E_{\alpha,\alpha+1-\hat{\alpha}}(At^\alpha) + A\Big(E_{\alpha,\alpha+1-\hat{\alpha}}(At^\alpha) - E_\alpha(At^\alpha)\Big) =: J_1 + J_2.\end{aligned}$$

Here handling the first term as in the proof of Theorem 2.3 gives, for $t > 1$ and $T > e$, that

$$|A|\Big|t^{\alpha-\hat{\alpha}} - 1\Big|E_{\alpha,\alpha+1-\hat{\alpha}}(At^\alpha)| \lesssim |\alpha - \hat{\alpha}| \log T.$$

Similarly, continuity and boundedness properties of the Mittag–Leffler functions give

$$|A|\left|E_{\alpha,\alpha+1-\hat{\alpha}}(At^{\alpha}) - E_{\alpha}(At^{\alpha})\right| \lesssim |\alpha - \hat{\alpha}|$$

and hence

$$|I_1(t)| \lesssim |\alpha - \hat{\alpha}| \log T.$$

It remains to study $I_2(t)$. Since f is Hölder continuous by Lemma 2.5, we have

$$D^{\alpha} f(t) = \frac{1}{\Gamma(1-\alpha)} \frac{f(t) - f(0)}{t^{\alpha}} + \frac{\alpha}{\Gamma(1-\alpha)} \int_0^t \frac{f(t) - f(s)}{(t-s)^{1+\alpha}} ds.$$

Set

$$\hat{D}^{\alpha} f(t) = \frac{f(t) - f(0)}{t^{\alpha}} + \int_0^t \frac{f(t) - f(s)}{(t-s)^{1+\alpha}} ds.$$

Using the smoothness of the Gamma function $\Gamma(x)$ around true $\alpha \in (0,1)$, we obtain the following:

$$\begin{aligned}
&|(D^{\hat{\alpha}} - D^{\alpha}) f(t)| \\
&\leq \left| \frac{1}{\Gamma(1-\hat{\alpha})} - \frac{1}{\Gamma(1-\alpha)} \right| \frac{|f(t) - f(0)|}{t^{\alpha}} + \frac{1}{\Gamma(1-\alpha)} |\hat{D}^{\alpha} f(t) - \hat{D}^{\hat{\alpha}} f(t)| \\
&+ \left| \frac{\hat{\alpha}}{\Gamma(1-\hat{\alpha})} - \frac{\alpha}{\Gamma(1-\alpha)} \right| |\hat{D}^{\alpha} f(t) - \hat{D}^{\hat{\alpha}} f(t)| \\
&\lesssim |\hat{\alpha} - \alpha| |\hat{D}^{\alpha} f(t)| + |\hat{D}^{\alpha} f(t) - \hat{D}^{\hat{\alpha}} f(t)|.
\end{aligned}$$

Here, thanks to Lemma 2.5,

$$|\hat{D}^{\alpha} f(t)| \lesssim C_T^{\eta} T^{\gamma - \alpha},$$

thereby handling the first term. For the second term, applying Hölder continuity of f together with

$$\left| \frac{1}{t^{\alpha}} - \frac{1}{t^{\hat{\alpha}}} \right| \lesssim \frac{\log t}{t^{\alpha}} |\alpha - \hat{\alpha}|$$

yields

$$|(D^{\hat{\alpha}} - D^{\alpha}) f(t)| \lesssim C_T^{\eta} \log T |\alpha - \hat{\alpha}| T^{\gamma - \alpha}.$$

Thus, we obtain the following:

$$|I_2(t)| \lesssim C_T^{\eta} \log T |\alpha - \hat{\alpha}| T^{\gamma - \alpha}.$$

Collecting the estimates for $I_j(t)$, $j = 1, 2, 3, 4$ completes the proof. □

2.1. Estimation procedure in practice

Now, the estimation of σ directly follows by following the approach based in quadratic variations on short intervals presented in [16]. However, the estimation of (b, Θ) is based on the estimation of the mean and covariances of a (almost) stationary series η, as discussed in [16]. For this, we note that the error in $|\hat{\eta} - \eta|$ propagates as T increases, while the observed series length T has to increase in order to accurately estimate the mean and covariance of η. Together with Theorem 2.4 and the asymptotic behavior of estimators $(\hat{b}, \hat{\Theta})$, this allows us to explicitly determine how accurately (α, A) have to be

estimated (on short-time asymptotics) to obtain sufficient accuracy for the estimation of (b, Θ) based on large-time asymptotics.

We note that it might be infeasible to assume dense samples on short times together with long horizon observations $T \to \infty$. More sparse samples to estimate (α, A) can be tackled using the regression trick, see Remark 2.2. On the other hand, on long horizon time scales, sparse samples simply mean discretized versions of Ornstein–Uhlenbeck models, and estimation can be done using discrete versions of methodology described in [16]. Under short memory, such as in the case of the classical Ornstein–Uhlenbeck process, shorter time intervals $[0, T]$ are sufficient. However, in order to capture long memory effects, that is, slowly decaying correlations on large time lags, observations on a long time horizon are obviously required.

We also note that in practice, one typically would not directly observe V but an erroneous process $\tilde{V}_t = V_t + \epsilon_t$ instead. Using $\log(1 + x) \sim x$ for $x \sim 0$, it is straightforward to see that in the estimation α, an additional error term of magnitude $\frac{\epsilon_t}{1-V_t}$ is obtained, provided that the quantity converges to zero. This error term should be compared to t^α provided in (2.9). Similarly, by linearity, we would obtain an additional error term $t^{-\hat{\alpha}}\epsilon_t$ in the estimation of A and an additional error term $D^{\hat{\alpha}}\epsilon_t - \hat{A}\epsilon_t$ in the noise recovery. Depending on the asymptotic behavior and growth properties of ϵ_t, these lead to straightforward error estimates for the case of noisy observations, in conjunction with Theorem 2.3 and Theorem 2.4.

Finally, we note that our numerical implementation gives rise to an error arising from discretised fractional differentiation. However, this is already well-understood in the literature, for example, see [19] and references therein.

3. Numerical illustrations

In this section, we illustrate the performance of our approach in practice via simulated examples. In Section 3.1, we describe our simulation setting, while in Section 3.2, we present our results.

3.1. Simulations

We adopt the strategy to simulate sample paths of V from ([10, Section 3]; [14, Section 6]). Indeed, motivated by the definition (2.2), for a given discretization mesh with an interval length of Δt, one sets for $t = N\Delta t$

$$D^\alpha V(t) \approx \frac{(\Delta t)^{-\alpha}}{\Gamma(2-\alpha)} \sum_{k=0}^{N-1} [V((k+1)\Delta t) - V(k\Delta t)][(N-k)^{1-\alpha} - (N-k-1)^{1-\alpha}]. \tag{3.1}$$

In our simulations, we consider the noise G in the noise dynamics of (2.1) to be the fractional Brownian motion (fBm) B^H with Hurst index H, that is, B^H is a centered Gaussian process with $B^H_0 = 0$ and covariance

$$R(s,t) = \frac{1}{2}\left[t^{2H} + s^{2H} - |t-s|^{2H}\right].$$

Within this noise, the process V can be simulated through Algorithm 1. Figure 1 shows examples of simulated paths of V for different values of the parameters A and Θ.

Algorithm 1 Simulation of the fractional neuronal model

1: **Initialize** the parameters $\alpha, A, b, \Theta, \sigma, H$, the initial value V_0, the step size Δt, the maximum number of time steps N, and the number of paths M.

2: Set the seed of the random number generator.

3: **Simulate the OU process** $\eta(t)$ via an Euler–Maruyama discretization scheme. At time instants $0 = t_0 < t_{\Delta t} < t_{2\Delta t} < \cdots < t_{N\Delta t}$, simulate an fBm $B^H(t)$ and construct the path of $\eta(t)$ by setting $\eta(0) = 0$, $B^H(0) = 0$, and

$$\eta(n\Delta t) = \eta((n-1)\Delta t) + \Theta\left(b - \eta((n-1)\Delta t)\right)\Delta t + \sigma\Big(B^H(n\Delta t) - B^H((n-1)\Delta t)\Big)$$

for $n = 1, \ldots, N$.

4: **Construct the path of** $V(t)$ at the same time instants by setting $V(0) = V_0$,

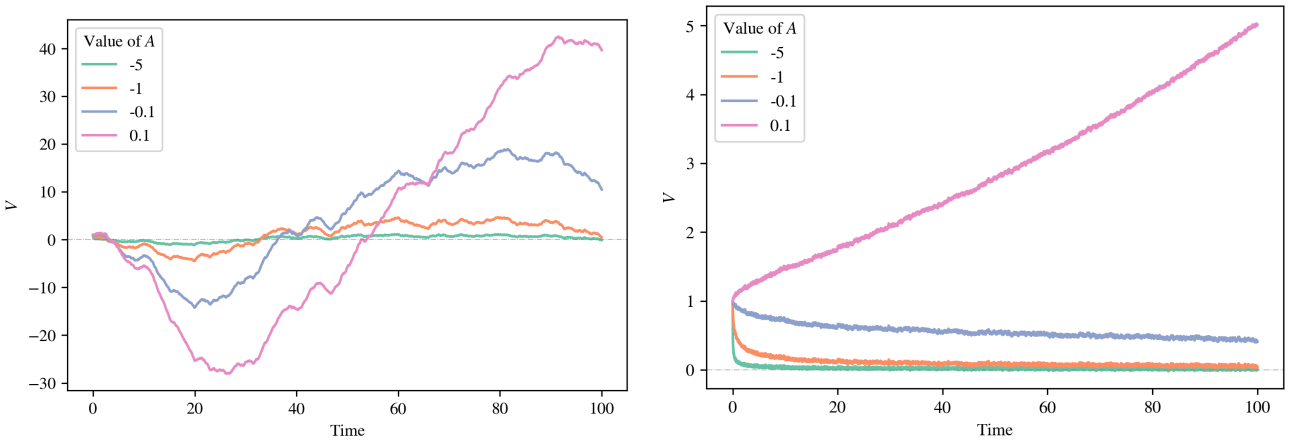
$$V(\Delta t) = V(0) + \frac{(\Delta t)^\alpha\,\Gamma(2-\alpha)}{2}\left(A\,V(0) + \eta(\Delta t)\right),$$

and applying the iterative scheme

$$\begin{aligned} V(n\Delta t) = {} & V((n-1)\Delta t) \\ & - \sum_{k=0}^{n-2}\left[V((k+1)\Delta t) - V(k\Delta t)\right]\left[(n-k)^{1-\alpha} - (n-k-1)^{1-\alpha}\right] \\ & + (\Delta t)^\alpha\,\Gamma(2-\alpha)\left(A\,V((n-1)\Delta t) + \eta(n\Delta t)\right) \end{aligned}$$

for $n = 2, \ldots, N$.

5: Repeat Steps 2–4 a total of M times, setting a new seed for the random number generator at each repetition.



(a) $\Theta = 0.1$. **(b)** $\Theta = 100$.

Figure 1. Simulated paths of V for different values of A and Θ.

3.2. Estimation

We present simulated examples to illustrate the performance and applicability of the proposed estimators. The simulations were performed using computer resources within the Aalto University School of Science "Science-IT" project.

For the estimation of α and A, many observations very close to 0 are required, whereas the estimation of Θ and σ requires observations within a long time period. Due to computational constraints, it is not feasible to work with a very long time series with extremely dense observations; however, in practice, one would sample more densely during a short interval in the beginning and then collect a longer time series with less dense observations. To mimic this practical approach, we simulated two separate paths of V for each sample: one on the time interval $[0, 0.001]$ with 10,000 observations, and another on the time interval $[0, 400]$ with 10,000 observations. The first part exhibits asymptotic behavior close to 0 and is used to estimate α and A, and the second part shows long-term behavior and is used to estimate Θ and σ.

We present two different simulated examples. In the first example, we set $b = 0$ and focus on the estimation of $(\alpha, A, \Theta, \sigma)$. The simulations were performed using the approach presented in Section 3.1 and the simulation parameters for the first example are given in Table 1. In the table, V_0 denotes the initial value of the process V. The process G in the noise process η was a fractional Brownian motion with the Hurst index H. In the examples, the values of α and H were varied while other parameters were kept constant. In total, 400 samples were simulated for each set of parameter values.

Table 1. Parameter values for simulations.

Parameter	Value	Parameter	Value	Parameter	Value
A	-0.1	Θ	5	T	400
b	0	σ	1	n	10000
α	{0.5, 0.7}	H	{0.5, 0.6, 0.7, 0.8}	V_0	1

The parameters α and A were estimated from the first part of each sample using the regression

method from Remark 2.2 and (2.6). After estimating α and A, the noise process η was recovered from the longer time series, and the parameters Θ and σ were estimated using the methods of [16]. Table 2 lists summary statistics for all estimated parameters in different test cases (different values of α and H).

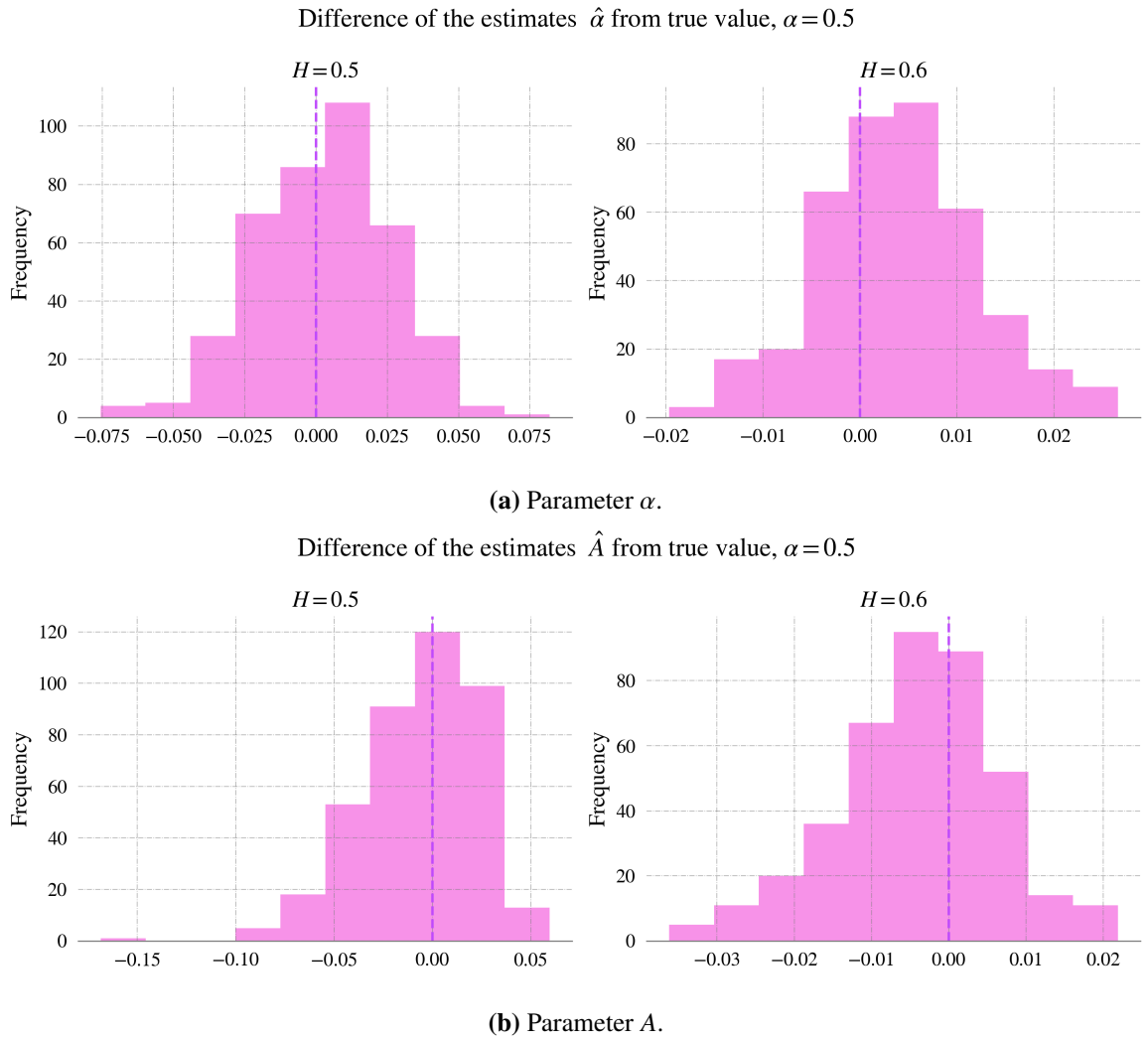
Table 2. Bias, standard deviation (SD), and root mean square error (RMSE) of the estimators for different values of α and H in the case $b = 0$. For Θ, the values in parentheses correspond to the estimates computed from the true noise.

		$\hat{\alpha}$			$\hat{A}$			$\hat{\Theta}$			$\hat{\sigma}$		
α	H	Bias	SD	RMSE	Bias	SD	RMSE	Bias	SD	RMSE	Bias	SD	RMSE
0.5	0.5	0.003	0.023	0.024	-0.006	0.030	0.030	0.272 (0.240)	0.444 (0.271)	0.520 (0.362)	0.032	0.042	0.052
0.5	0.6	0.004	0.008	0.009	-0.004	0.010	0.011	0.136 (0.079)	0.295 (0.272)	0.325 (0.284)	0.017	0.014	0.022
0.7	0.7	0.005	0.003	0.006	-0.005	0.004	0.006	-0.054 (-0.116)	0.318 (0.310)	0.323 (0.332)	-0.009	0.006	0.010
0.7	0.8	0.005	0.001	0.005	-0.005	0.001	0.006	-0.333 (-0.382)	0.382 (0.372)	0.506 (0.534)	-0.059	0.004	0.059

The case $\alpha = 0.5$ was simulated with two different noise processes: standard Brownian motion ($H = 0.5$) and fBm with a Hurst index of 0.6. The case $\alpha = 0.5$ and $H = 0.5$ is not covered by Theorem 2.4, which requires that $H > \alpha$. However, we include this case in the empirical examples to illustrate the boundary behavior of our approach. Figure 2 displays the differences of the estimates $\hat{\alpha}$ and $\hat{A}$ from their true values as histograms. The first column of the figure corresponds to the case when $H = 0.5$ and the second column to $H = 0.6$. Based on the histograms, it seems that the parameters α and A could be well estimated from the simulated data with both noise processes. All histograms are centered at 0, but for a larger H, the histograms appear wider. This is due to the differences in the correlation structures of η with different Hurst indices.

Figure 3 shows the differences of the estimates $\hat{\Theta}$ computed from the recovered noise $\hat{\eta}$ and the true value Θ as histograms for the case $\alpha = 0.5$. For comparison, the parameter Θ was also estimated from the true noise η, yielding estimates $\hat{\Theta}_{\text{true noise}}$ for each sample. Moreover, the figure shows the difference of the estimates $\hat{\Theta}_{\text{true noise}}$ from the true parameter Θ as histograms. Based on the histograms, Θ could be well estimated from the data. The histograms corresponding to the estimates from recovered noise (left column of the figure) are slightly wider than the histograms corresponding to true noise. Similarly, Table 2 shows that both the standard deviation (SD) and the root mean square error (RMSE) of $\hat{\Theta}$ are larger than the SD and RMSE of $\hat{\Theta}_{\text{true noise}}$. However, it seems that the noise recovery works sufficiently well and does not make too large an error. The parameter σ could be estimated equally well from the data, as can be seen in Figure 6a, which shows the differences between the estimates of σ and the true value of the parameter in the case $\alpha = 0.5$. The estimates for σ were computed from $\hat{\eta}$.

For the case $\alpha = 0.7$, simulations were run with two different fractional Brownian motions as the noise process, corresponding to Hurst indices $H = 0.7$ and $H = 0.8$. Again, the case $\alpha = H = 0.7$ where α and H are equal is not covered by Theorem 2.4, but we present it here nevertheless. Figure 4 displays the differences between the estimates of α and A from their true values for different values of H when $\alpha = 0.7$. The histograms seem to be slightly shifted from 0, especially in the case $H = 0.8$. However, the scale of the horizontal axis of the histograms is, for both $H = 0.7$ and $H = 0.8$, considerably smaller than in the previous examples with $\alpha = 0.5$. Therefore, it seems that as α increases, the estimates of α and A get more accurate, even though there appears to be a slight bias in the estimates. This phenomenon can be observed in Table 2: as α increases, the RMSE of $\hat{\alpha}$ and $\hat{A}$ decrease but the



(a) Parameter α.

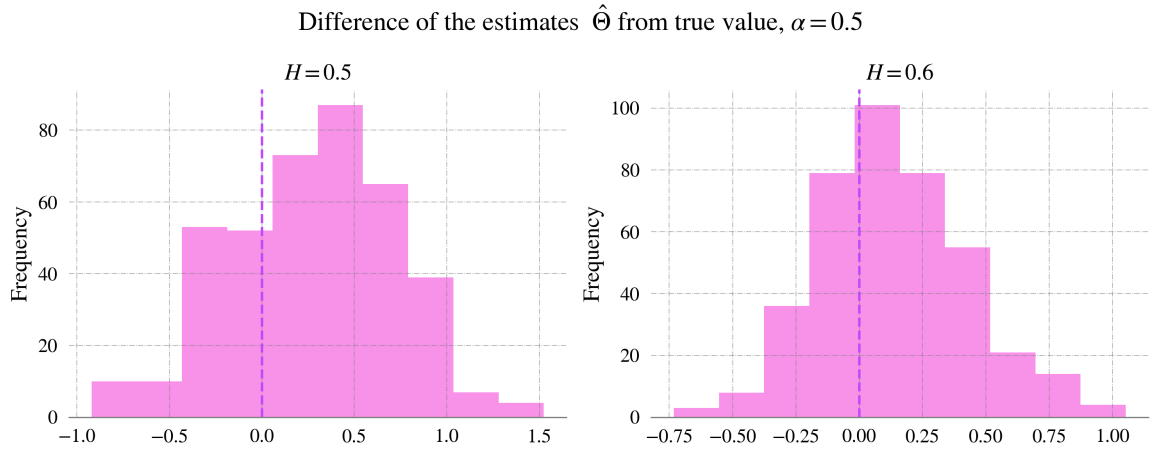
(b) Parameter A.

Figure 2. Differences between parameter estimates and true values of the parameters α and A for different values of H when $\alpha = 0.5$.

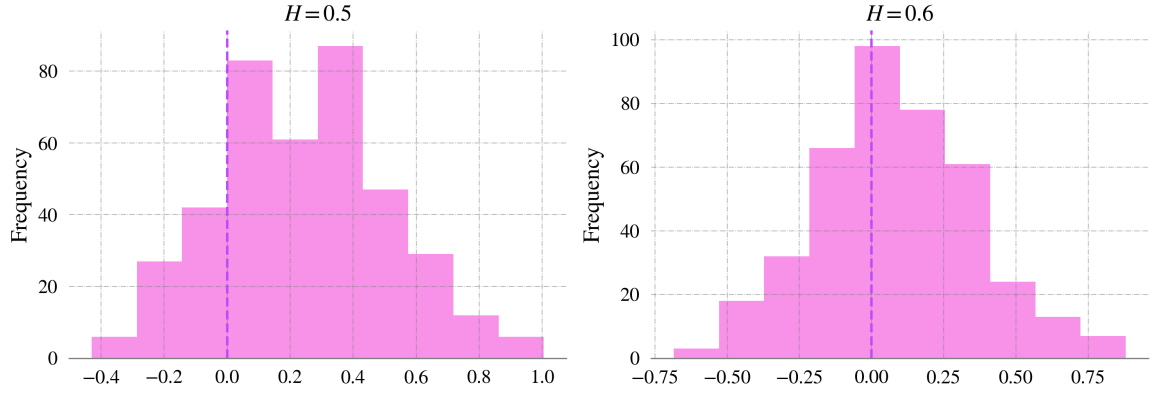
bias of $\hat{\alpha}$ slightly increases.

Figure 5 displays the differences of the estimates $\hat{\Theta}$, computed from recovered noise, and the estimates $\hat{\Theta}_{\text{true noise}}$, computed from true noise, from the true value Θ as histograms for the case $\alpha = 0.7$. Based on the histograms, Θ could be well estimated from the data in this case, too. Now, the histograms corresponding to estimates from recovered noise look very similar to the histograms corresponding to estimates from true noise for both values of H. The histograms corresponding to recovered noise are still slightly wider than the histograms corresponding to true noise, but this phenomenon is less visible than in the case $\alpha = 0.5$. For example, in the case $\alpha = 0.7$ and $H = 0.7$, the standard deviations of $\hat{\Theta}$ and $\hat{\Theta}_{\text{true noise}}$ are 0.318 and 0.310, respectively, whereas in the case $\alpha = 0.5$ and $H = 0.5$, the standard deviations are 0.444 for $\hat{\Theta}$ and 0.271 for $\hat{\Theta}_{\text{true noise}}$. The reason for this is that when $\alpha = 0.7$, the parameters α and A could be estimated more accurately, resulting in the recovered noise being closer to the true noise.

Figure 6b displays the histograms of the differences between the estimates $\hat{\sigma}$ and the true value σ



(a) Estimates $\hat{\Theta}$ computed from estimated noise.

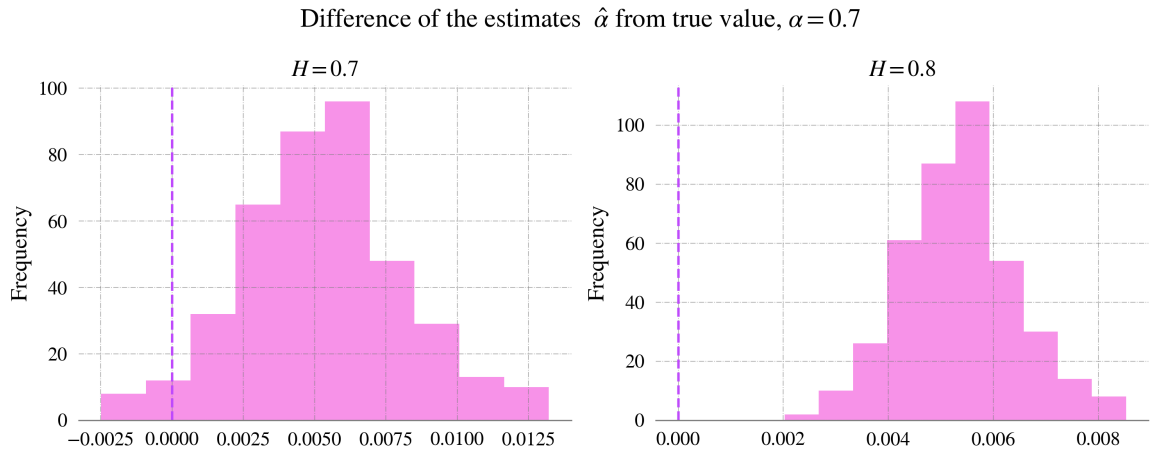


(b) Estimates $\hat{\Theta}_{\text{true noise}}$ computed from true noise.

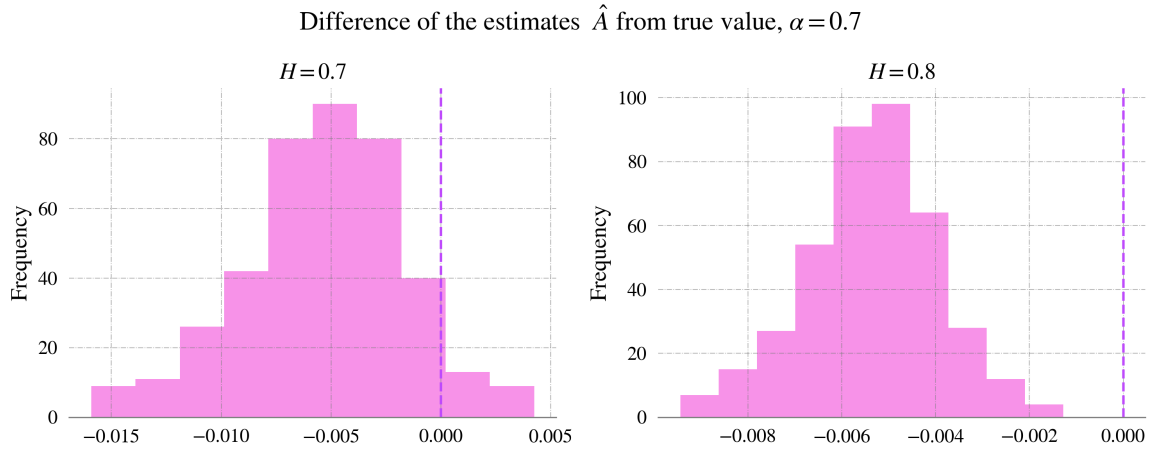
Figure 3. Differences between parameter estimates and true values of the parameter Θ for different values of H when $\alpha = 0.5$.

in the case $\alpha = 0.7$. There is a noticeable bias in the estimates, especially when $H = 0.8$. Additionally, Table 2 shows a small standard deviation but a larger magnitude of bias for $\hat{\sigma}$ in this case. This is aligned with the theoretical error provided in Theorem 2.4 suggesting larger error if H increases compared to α. However, the magnitude of the bias is small compared to the true value of the parameter (around 1 % for $H = 0.7$ and 6 % for $H = 0.8$), meaning that the parameter could be estimated well. The same phenomenon was observed in [16].

In the second simulated example, we set $b = 3$ and kept other simulation parameters the same as in the first example. This example was conducted for the case $\alpha = 0.5$, $H = 0.6$. Overall, the estimates in the second example were good (see Table 3 for the summary statistics of all estimators). The constant term $b = 3$ does not affect the asymptotic behavior of V near zero, so the estimation of α and A performed nearly identically to the case with $b = 0$. Figure 7 displays the differences between the estimates of b and Θ and their true values as histograms. Based on the figure, both parameters could be estimated well from the data. Furthermore, the RMSE of $\hat{\Theta}$ is of similar magnitude to the



(a) Parameter α.



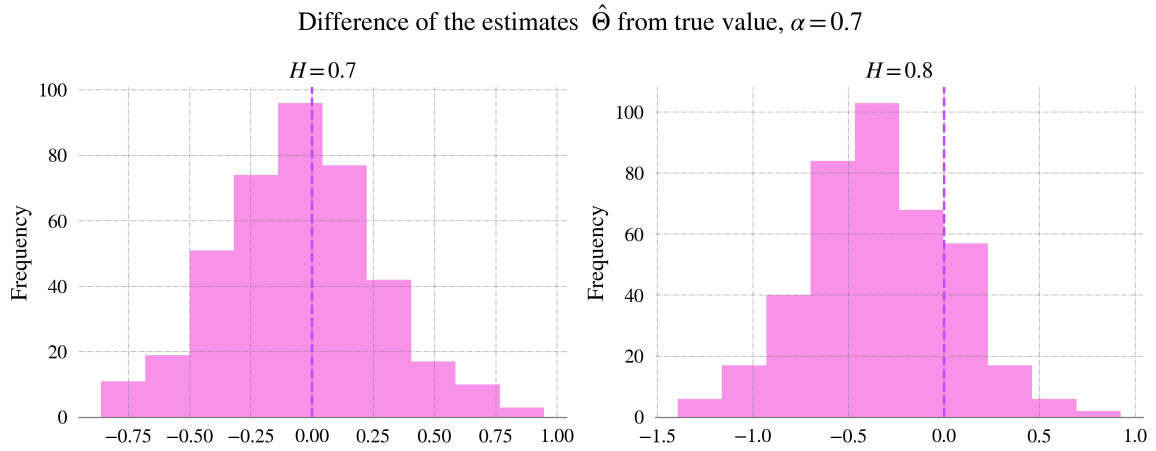
(b) Parameter A.

Figure 4. Differences between parameter estimates and true values of the parameters α and A for different values of H when $\alpha = 0.7$.

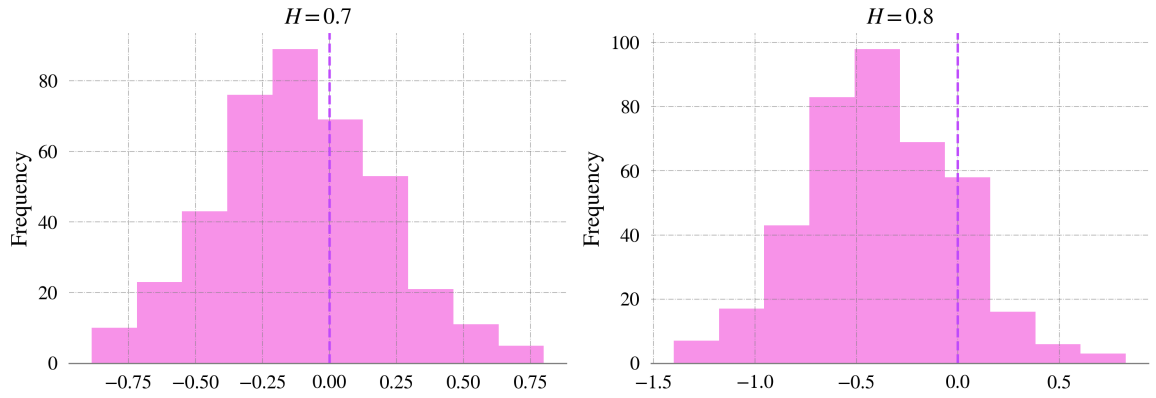
RMSE values obtained in the first example.

4. Conclusions

In this article, we investigated a generalized stochastic fractional neuronal model combining fractional dynamics with correlated stochastic inputs. The proposed framework extends several classes of fractional neuronal systems previously introduced in the literature and incorporates, within a unified setting, both hereditary effects induced by fractional differentiation and temporal dependence generated by stochastic processes with stationary increments. More precisely, the model couples a fractional differential equation for the neuronal state variable with a latent mean-reverting stochastic process describing correlated external inputs. This formulation allows one to reproduce nonlocal temporal behavior, persistent correlations, and non-exponential relaxation phenomena which are frequently observed in biological and neuronal systems and which cannot be adequately captured within classical



(a) Estimates $\hat{\Theta}$ computed from estimated noise.



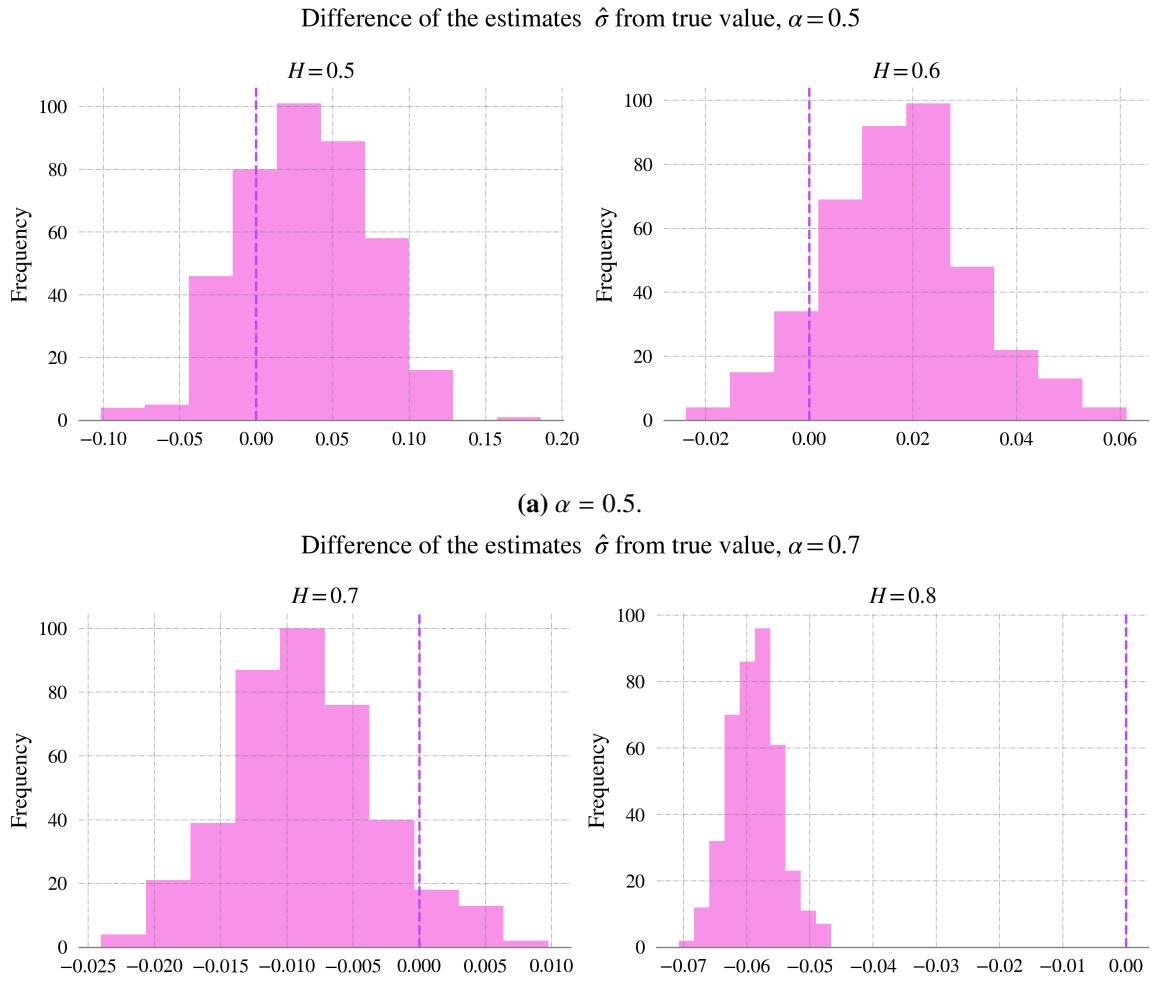
(b) Estimates $\hat{\Theta}_{\text{true noise}}$ computed from true noise.

Figure 5. Differences between parameter estimates and true values of the parameter Θ for different values of H when $\alpha = 0.7$.

Markovian approaches.

The main purpose of the article was not only the introduction of the model itself, but also the development of a feasible statistical methodology for parameter estimation. For this, we have proposed a two-step estimation procedure. First, the parameters governing the fractional dynamics were estimated through asymptotic properties of the Mittag–Leffler solution near the origin. Then, after reconstruction of the latent stochastic input through fractional differentiation, the parameters of the hidden noise dynamics were estimated by means of inference techniques for generalized Ornstein–Uhlenbeck type processes.

From the theoretical viewpoint, the analysis highlighted the delicate interplay between the regularity of the driving noise and the order of the fractional derivative. In particular, the condition $\alpha < \gamma$ naturally appeared in the study of the reconstruction error of the latent process when the driving noise possesses γ-Hölder continuous trajectories. Under this regime, the fractional differentiation operator remained sufficiently stable with respect to small perturbations of the estimated fractional parameter, allowing a



(a) $\alpha = 0.5$.

(b) $\alpha = 0.7$.

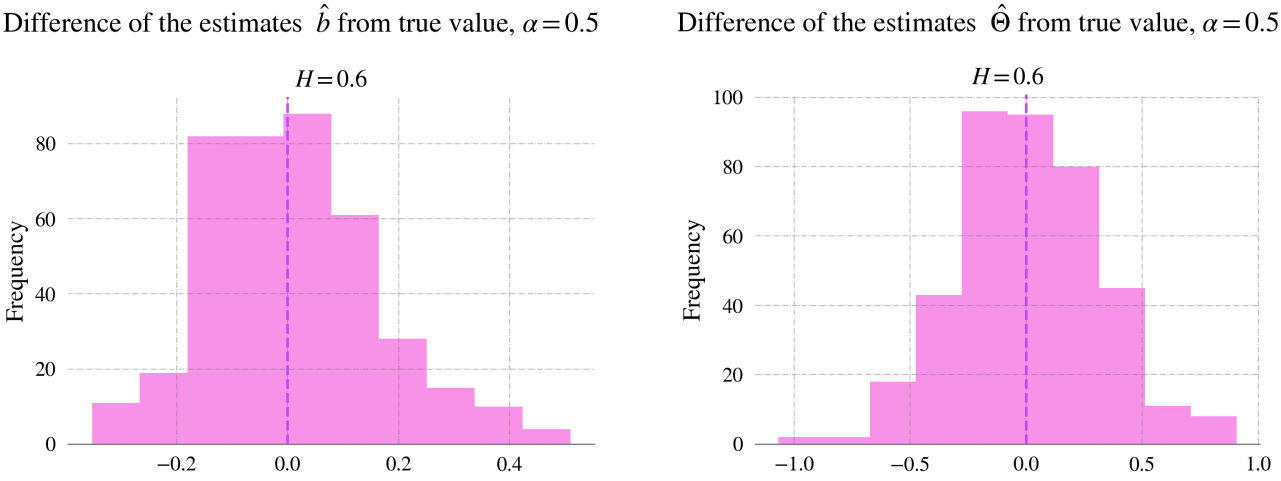
Figure 6. Differences between the estimates of σ from the true value for different values of α and H.

consistent reconstruction of the hidden stochastic component on compact intervals.

The numerical experiments confirmed the practical applicability of the proposed methodology. The estimation procedure for the parameters α and A performed well when sufficiently many observations close to the origin were available, which is consistent with the asymptotic structure of the solution. Moreover, the recovery of the latent noise process appeared sufficiently accurate to allow for the subsequent estimation of the parameters Θ and σ governing the hidden dynamics. At the same time, the simulations also revealed intrinsic difficulties associated with non-Markovian models with memory. In particular, the quality of the estimation of Θ and σ deteriorated as the regularity parameter H increased, reflecting the stronger dependence structure of the driving noise. More generally, the analysis suggested that the reconstruction error of the latent process may accumulate over long time intervals, while reliable estimation of covariance-based quantities requires large observation horizons. This creates a nontrivial balance between local estimation near the origin and long-time statistical inference. Repeating the experiments with varying step sizes, time horizons and numbers of observations would

Table 3. Bias, SD, and RMSE of the estimators in the case $b = 3$ with $\alpha = 0.5$, $H = 0.6$. For Θ, the values in parentheses correspond to the estimates computed from the true noise.

	$\hat{\alpha}$	$\hat{A}$	$\hat{b}$	$\hat{\Theta}$	$\hat{\sigma}$
Bias	0.001	0.000	0.007	0.011 (0.079)	0.012
SD	0.008	0.010	0.151	0.310 (0.272)	0.014
RMSE	0.008	0.010	0.151	0.310 (0.284)	0.019



(a) Parameter b.

(b) Parameter Θ.

Figure 7. Differences between parameter estimates and true values of the parameters b and Θ when $\alpha = 0.5$ and $H = 0.6$ in the case $b = 3$.

provide important information about the robustness of the proposed approach. Furthermore, the estimation procedure could be tested by applying it to real data and analyzing the results in different settings.

From a broader perspective, the present work further supports the relevance of fractional stochastic analysis in mathematical neuroscience. The combination of fractional operators, correlated stochastic forcing, and latent-variable inference provides a flexible and mathematically rich framework for modeling systems with memory and complex temporal organization. In this regard, the ideas developed may stimulate further research at the intersection of fractional calculus, stochastic analysis, statistical inference, and neuronal modeling. As simple examples of open remaining problems, it would be interesting to study exact asymptotic analysis of the estimators and reconstructed noise process. Another natural extension concerns multidimensional neuronal systems and interacting network models, where both the state dynamics and the latent noise process are vector-valued. Finally, we restricted our analysis to the case $\gamma > \alpha$. It would be interesting to examine what happens in the regime $\gamma \leq \alpha$.

Use of AI tools declaration

The authors declare they have not used Artificial Intelligence (AI) tools in the creation of this article.

Acknowledgments

P. Ilmonen and M. Laurikkala gratefully acknowledge support from the Research Council of Finland via Finnish Centre of Excellence in Randomness and Structures (decision number 346308). M. Laurikkala gratefully acknowledges support from Emil Aaltonen Foundation (grant number 250110 K1). This study was also partially funded by the projects PRIN2022-MUR 2022XZSAFN and PRIN-PNRR P2022XSF5H.

Conflict of interest

Enrica Pirozzi is a special issue editor for Mathematical Biosciences and Engineering and was not involved in the editorial review or the decision to publish this article. All authors declare that there are no competing interests.

References

1. H. C. Tuckwell, *Introduction to Theoretical Neurobiology*, Cambridge University Press, Cambridge, 1988. https://doi.org/10.1017/cbo9780511623202
2. L. Sacerdote, M. T. Giraudo, Stochastic integrate and fire models: A review on mathematical methods and their applications, In *Stochastic Biomathematical Models, Lecture Notes in Mathematics*, Springer, Heidelberg, (2013), 99–148. https://doi.org/10.1007/978-3-642-32157-3_5
3. C. Siettos, J. Starke, Multiscale modeling of brain dynamics: From single neurons and networks to mathematical tools, *WIRES Syst. Biol. Med.*, **8** (2016), 438–458. https://doi.org/10.1002/wsbm.1348
4. R. L. Magin, *Fractional Calculus in Bioengineering*, Begell House Publishers, Connecticut, 2006.
5. F. Mainardi, *Fractional Calculus and Waves in Linear Viscoelasticity*, Imperial College Press, London, 2010. https://doi.org/10.1142/p614
6. M. M. Meerschaert, A. S. Sikorskii, *Stochastic Models for Fractional Calculus*, De Gruyter, Berlin, 2012. https://doi.org/10.1515/9783110258165
7. R. Metzler, J. Klafter, The random walk's guide to anomalous diffusion: a fractional dynamics approach, *Phys. Rep.*, **339** (2000), 1–77. https://doi.org/10.1016/S0370-1573(00)00070-3
8. E. Pirozzi, Some Fractional Stochastic Models for Neuronal Activity with Different Time-Scales and Correlated Inputs, *Fract. Fract.*, **8** (2024), 57. https://doi.org/10.3390/fractalfract8010057
9. W. Teka, T. M. Marinov, F. Santamaria, Neuronal spike timing adaptation described with a fractional leaky integrate-and-fire model, *PLoS Comput. Biol.*, **10** (2014), e1003526. https://doi.org/10.1371/journal.pcbi.1003526
10. E. Pirozzi, Colored noise and a stochastic fractional model for correlated inputs and adaptation in neuronal firing, *Biological Cybernetics*, **112** (2018), 25–39. https://doi.org/10.1007/s00422-017-0731-0
11. M. Abundo, E. Pirozzi, Fractionally integrated Gauss–Markov processes and applications, *Commun. Nonlinear Sci Numer. Simul.*, **101** (2021), 105862. https://doi.org/10.1016/j.cnsns.2021.105862

12. E. Pirozzi, Mittag–Leffler fractional stochastic integrals and processes with applications, *Mathematics*, **12** (2024), 3094. https://doi.org/10.3390/math12193094
13. M. M. Meerschaert, P. Straka, Inverse stable subordinators, *Math. Model. Nat. Phenom.*, **8** (2013), 1–16. https://doi.org/10.1051/mmnp/20138201
14. N. Leonenko, E. Pirozzi, The time-changed stochastic approach and fractionally integrated processes to model the actin–myosin interaction and dwell times, *Math. Biosci. Eng.*, **22** (2025), 1019–1054. https://doi.org/10.3934/mbe.2025037
15. M. Voutilainen, L. Viitasaari, P. Ilmonen, S. Torres, C. Tudor, Vector-valued generalised Ornstein–Uhlenbeck processes: properties and parameter estimation, *Scand. J. Stat.*, **49** (2022), 992–1022. https://doi.org/10.1111/sjos.12552
16. P. Ilmonen, M. Laurikkala, K. Ralchenko, T. Sottinen, L. Viitasaari, Data driven modeling of multiple interest rates with generalized Vasicek-type models, *arXiv preprint arXiv:2509.03208*, 2025. https://arxiv.org/abs/2509.03208
17. A. N. Burkitt, A review of the integrate-and-fire neuron model: I. homogeneous synaptic input, *Biol. Cybern.*, **95** (2006), 1–19. https://doi.org/10.1007/s00422-006-0068-6
18. R. Gorenflo, A. A. Kilbas, F. Mainardi, S. Rogosin, *Mittag-Leffler Functions, Related Topics and Applications*, Springer, Berlin, 2020. https://doi.org/10.1007/978-3-662-61550-8
19. S. G. Samko, A. A. Kilbas, O. I. Marichev, *Fractional Integrals and Derivatives: Theory and Applications*, Gordon and Breach Science Publishers, Amsterdam, 1993.



AIMS Press

© 2026 the Author(s), licensee AIMS Press. This is an open access article distributed under the terms of the Creative Commons Attribution License (https://creativecommons.org/licenses/by/4.0)